

---

**Cardiac Gated Blood Pool Study: Rest (Tc-99m-Red Blood Cells)**

**Overview** The resting Cardiac Gated Blood Pool Study provides information about pulmonary blood flow during the first circulation of the radiopharmaceutical, and then, after equilibration of the radiopharmaceutical, it provides information about cardiac chamber volumes, including ejection fraction, as a function of the cardiac cycle.

**Radiopharmaceutical characteristics** The Tc-99m-red blood cell is one of the largest radiopharmaceuticals with a diameter of approximately 8  $\mu\text{m}$ , a thickness of approximately 2  $\mu\text{m}$ , and a central thickness of approximately 1  $\mu\text{m}$  (Fig. 12.1) [1].

**Extraction mechanism** None. The Tc-99m-red blood cells are confined to the vascular space. The diameter of a capillary is similar to that of a red blood cell so that the red blood cells pass through the capillaries in a single file.

**Extraction efficiency** 0 %.

**Extraction mechanism, saturable or non-saturable** N/A.

**Interventions** None.

**Imaging** Gamma camera planar imaging is most commonly used. Some institutions use gamma camera SPECT or SPECT-CT.

**Protocol design** The vascular space is labeled by injecting Tc-99m-red blood cells intravenously. The protocol consists of two parts, acquisition of sequential 1 s images for 30 s during the first circulation beginning at the time of injection and acquisition of delayed gated images of the heart in the anterior, left anterior oblique, and left lateral projections. It takes an average of 20 s for a red blood cell to complete one cycle through the vascular system, so, in conjunction with laminar flow and mixing in the cardiac chambers, equilibrium is achieved quickly.

Acquisition of the images of the left ventricle at various phases throughout the cardiac cycle requires a special technique. Normally planar images are acquired from 1 to 5 min in order to record enough counts to have reasonable statistics in the image. However, a cardiac cycle lasts only about 1 s and optimal temporal

**Fig. 12.1** Scanning electron micrograph of human red blood cell (From Freedman [1])

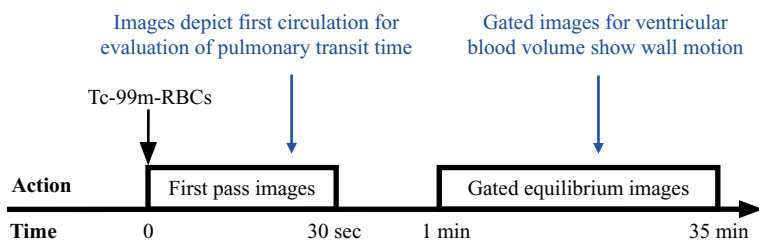
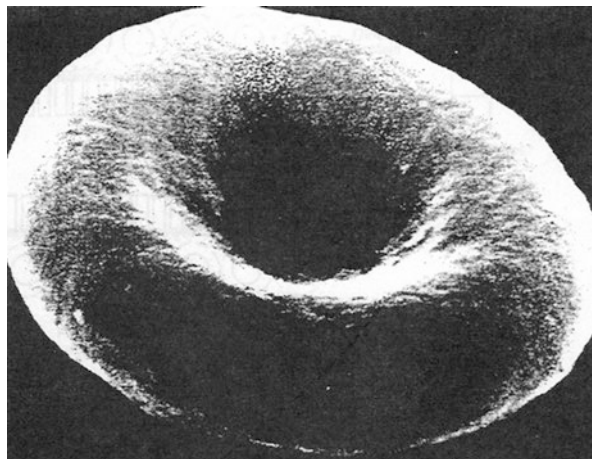


**Fig. 12.2** Protocol summary diagram

resolution during the cardiac cycle requires approximately 16 images. Thus, it is impossible to record enough counts for statistical reliability in each of 16 images during one cardiac cycle.

This problem is solved by attaching electrocardiograph (EKG) leads to the patient and sending the EKG signal to a computer that records the incoming counts from the gamma camera. The computer assigns incoming counts to the 16 images depending on the elapsed time since the last Q wave. After approximately 600 s or 10 min, there is an appropriate number of counts in each of the 16 images (Fig. 12.2).

**Quantitative measurement (visual): Pulmonary transit time** The pulmonary transit time is evaluated by a simple index, the time it takes for the leading edge of the first circulation bolus to pass from the right ventricle to the left ventricle. Specifically, it is the difference in time from the first appearance of the bolus in the right ventricle to the first appearance of the bolus in the left ventricle. The conceptual equation is,

$$\bar{T}(\text{sec}) = \frac{V(\text{mL})}{F(\text{mL}/\text{sec})} \approx T_{LE}(\text{sec}) \quad (12.1)$$

Here the central volume principle equation (see Chap. 5, Mean Transit Time: Central Volume Principle) has been solved for mean transit time instead of flow.  $\bar{T}$  represents the mean transit time of blood flow through the pulmonary arterial circulation,  $V$  represents pulmonary blood volume, and  $F$  represents pulmonary blood flow. However, since the pulmonary blood volume and blood flow cannot be easily determined, the mean transit time cannot be calculated. Instead, the leading edge transit time,  $T_{LE}$ , is used as an index of the mean transit time. Because of laminar flow, the leading edge transit time will always be shorter than the mean transit time.

**Pulmonary transit time: normal values** The leading edge pulmonary transit time should not exceed 6 s. Greater values indicate an increased pulmonary blood volume and/or a decreased pulmonary blood flow. The most common cause of a prolonged leading edge pulmonary transit time is left ventricular failure, which causes both an increase in pulmonary blood volume and a decrease in pulmonary blood flow secondary to a decrease in cardiac output.

**Quantitative measurement: left ventricular ejection fraction** The left ventricular ejection fraction, a key measure of cardiac function, is an example of relative quantification in nuclear medicine images in that it is unrelated to the amount of radiopharmaceutical that was administered (see Chap. 8, Quantitation of Function: Relative Measurements).

Since there is little change in photon attenuation between the end diastolic and end systolic images of the left ventricle, and since the left ventricular ejection fraction is a relative measurement, there is no need to know the absolute amount of activity in the left ventricle and attenuation correction is unnecessary.

However, since there is significant activity in the tissues around the left ventricle, background correction is needed. Figure 12.3 shows a planar image of the heart from the LAO projection (adjusted to optimize the separation between the left and right ventricles) with a region of interest (ROI) over the left ventricle and a background ROI over the lower left lung. The background ROI must not overlap the left ventricle, even at end diastole. The equation for background correction of an ROI is given in Chap. 8 as Eq. 8.3 and is not reproduced here.

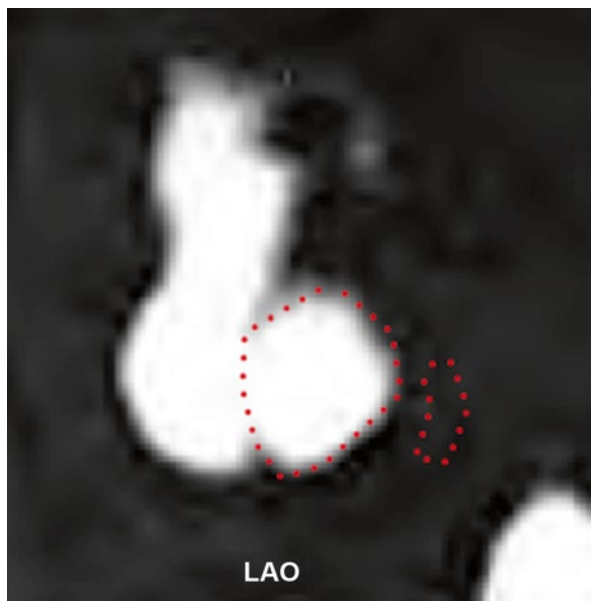
The equation for left ventricular ejection fraction, after the end diastolic and end systolic ROIs are corrected for background activity, is simply

$$EF_{LV} (\%) = \frac{LV_{ED} (cts) - LV_{ES} (cts)}{LV_{ED} (cts)} \times 100 (\%) \quad (12.2)$$

Here, “ $EF_{LV} (\%)$ ” is the left ventricular ejection fraction in percent, “ $LV_{ED} (cts)$ ” is the background corrected counts in the left ventricle at end diastole, and “ $LV_{ES} (cts)$ ” is the background corrected counts in the left ventricle at end systole.

The same approach can be used to evaluate the right ventricular ejection fraction. With planar imaging, there is some unavoidable overlap of the ventricle and corresponding atrium, which is not corrected for. However, the Cardiac Gated Blood Pool Study may be performed with SPECT or SPECT-CT [6]. SPECT eliminates the need for background correction, and SPECT-CT also corrects for photon

**Fig. 12.3** Left anterior oblique (LAO) cardiac gated blood pool image of the heart. ROIs have been placed over the left ventricle for left ventricular volume counts and lower left lung for background counts (Corbett et al. [5])



attenuation, but there is relatively little increase in accuracy of the ejection fraction measurement [2]. The same concepts and equation are used to calculate the gallbladder ejection fraction in the Hepatobiliary Study (see Chap. 15, Gastrointestinal System).

**Left ventricular ejection fraction: normal values** See Table 12.1 [3, 4]. Values are given where values could be identified in the literature separately for males and females. At the same time, there are many published studies confirming a strong correlation between measurement of the left ventricular ejection fraction in various nuclear medicine studies and measurement of the left ventricular ejection fraction by CT or MRI. Females have a smaller left ventricle than males and a slightly higher ejection fraction. This results in a lower cardiac reserve.

---

## Lymphoscintigraphy (Filtered Tc-99m-Sulfur Colloid)

**Overview** The Lymphoscintigraphy Study demonstrates the flow of lymph from the site of injection into the interstitial space through the draining lymphatics to the sentinel lymph node(s).

**Radiopharmaceutical characteristics** The commercially available Tc-99m-sulfur colloid that is injected intravenously contains colloidal particles that are too large to easily pass through the interstitial spaces. Therefore, the commercial Tc-99m-sulfur colloid is filtered prior to injection for lymphoscintigraphy. The filtration process reduces the maximum colloidal particle size from 5.0 to 0.22  $\mu\text{m}$  [6].

**Table 12.1** Normal values for quantitative parameters

Parameter	Working Normal range	Actual Normal range	References
<i>Cardiac gated blood pool study</i>			
Leading edge pulmonary transit time	≤6 s	–	–
Ejection fraction (rest) – male	50–75 %	48–72 %	[3, 4]
Ejection fraction (rest) – female	–	–	–
<i>Myocardial perfusion study – N-13-ammonia</i>			
Ejection fraction (rest) – male and female	50–75 %	49–73 %	[10]
<i>Myocardial perfusion study – Rb-82-rubidium</i>			
Ejection fraction (rest) – male	–	–	–
Ejection fraction (rest) – female	40–70 %	40–68 %	[14]
Ejection fraction (stress) – male	–	–	–
Ejection fraction (stress) – female	50–75 %	50–74 %	[14]
<i>Myocardial perfusion study – Tc-99 m-sestamibi</i>			
Ejection fraction (<45 years, rest) – male	45–65 %	45–65 %	[20]
Ejection fraction (<45 years, rest) – female	40–75 %	41–73 %	[20]
Ejection fraction (45–65 years, rest) – male	45–70 %	47–71 %	[20]
Ejection fraction (45–65 years, rest) – female	45–80 %	47–81 %	[20]
Ejection fraction (>65 years, rest) – male	45–75 %	46–74 %	[20]
Ejection fraction (>65 years, rest) – female	55–85 %	56–86 %	[20]
<i>Myocardial perfusion and viability – Tl-201</i>			
Ejection fraction – male	45–75 %	45–73 %	[18]
Ejection fraction – female	50–85 %	51–83 %	[18]
<i>Myocardial viability – F-18-FDG</i>			
Ejection fraction – male	–	–	–
Ejection fraction – female	–	–	–

**Extraction mechanism** Filtered Tc-99m-sulfur colloid is cleared from the flowing lymph by the mechanism of phagocytosis by macrophages that line the sinusoids of lymph nodes (Fig. 12.4). (See Chap. 4, Evaluation of Clearance for a conceptual and mathematical discussion of clearance). Macrophages are relatively large cells measuring 20–30  $\mu\text{m}$  in diameter, much larger than the 7  $\mu\text{m}$  diameter of a capillary [6, 7]. When a circulating macrophage enters a capillary, it temporarily obstructs the capillary while it squeezes through the capillary to reach the venule. Since there is no blood flow through the capillary while the macrophage is blocking the lumen, no colloidal particles can flow past macrophages.

However, sinusoids, which are found in the liver, spleen, and bone marrow in the vascular system, and in the lymph nodes in the lymph system, are much larger than capillaries with a diameter of 30–40  $\mu\text{m}$  [6]. The macrophages adhere to the sides of the sinusoid, and the blood carrying the colloidal particles flows along the sides of the macrophages. This allows the colloidal particles to bind to the surface of the macrophages and to be phagocytized.

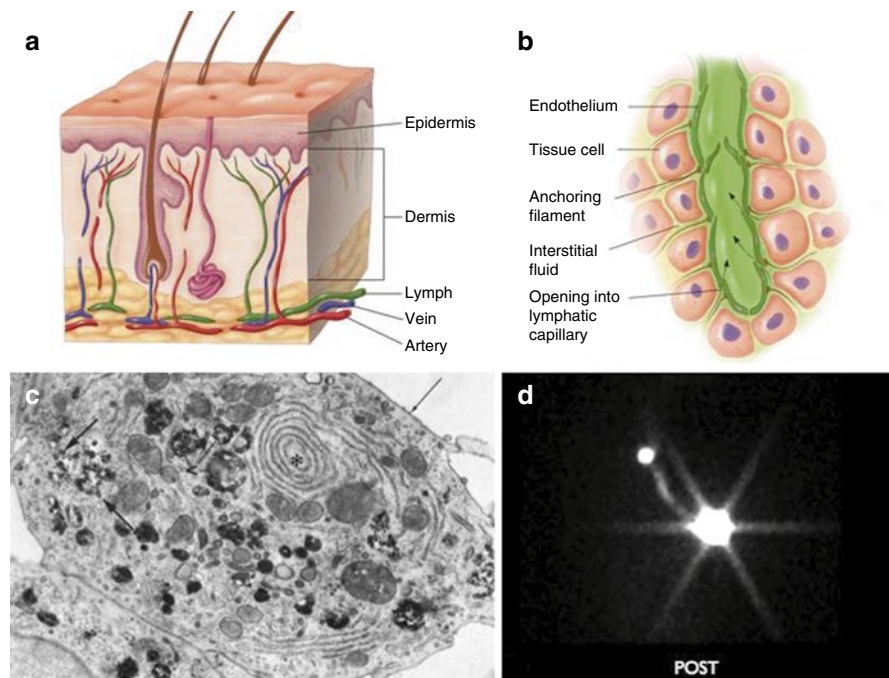


**Fig. 12.4** Biology of lymphoscintigraphy. (a, b) Diagrams of skin and terminal lymph vessel. Injection of sulfur colloid should be in the superficial dermis to maximize movement of colloid from the interstitium into lymphatic vessels. (c) Electron micrograph of a macrophage in a lymph node shows multiple vacuoles containing phagocytized carbon particles (From Nopajaroonsri and Simon [7], Fig 7, p 25). (d) Patient with melanoma upper left back. Tracer injection site is in the middle of an image with star-shaped artifacts. Lymph vessel is seen passing to focal uptake in a left axillary sentinel lymph node

**Extraction efficiency** The extraction efficiency of lymph nodes for colloid in general, including filtered Tc-99m-sulfur colloid, is high. From clinical experience, very little radiopharmaceutical passes through a sentinel lymph node to reach a second-tier lymph node during the typical duration of a lymphoscintigraphy study.

**Extraction mechanism, saturable or non-saturable** Non-saturable.

**Interventions** None.

**Imaging** Gamma camera planar imaging with a high-resolution, low-energy collimator is most commonly used. Some institutions use gamma camera SPECT or SPECT-CT, particularly in the case of complex anatomy, e.g., neck lymphoscintigraphy.

**Protocol design** The filtered Tc-99m-sulfur colloid is injected intradermally with a 30 gauge needle so as to produce a visible wheal. The location and duration of imaging depends on the purpose of the study. The delayed images are timed to show clearance of the tracer from lymph vessels into mononuclear phagocytes or macrophages (Fig. 12.5).

**Quantitative measurement** None.

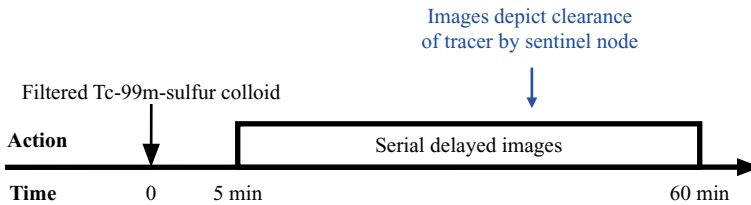


**Fig. 12.5** Protocol summary diagram

## Myocardial Perfusion Study (N-13-Ammonia)

**Overview** The Myocardial Perfusion Study with N-13-ammonia is used to evaluate the distribution of blood flow and perfusion to the myocardium at rest and stress [8]. In addition, the images are routinely gated to show regional wall motion and to allow calculation of the left ventricular ejection fraction.

Despite the fact that the title of the study says “myocardial perfusion,” the images actually reflect myocardial clearance. This is true of all of the nuclear medicine studies that have the word “perfusion” in the title. Relative clearance will reflect relative perfusion or blood flow as long as the extraction efficiency is uniform throughout the range of coronary blood flow that is being imaged, but this is not always the case. For example, the extraction efficiency is higher in myocardium at low flow rates than at high flow rates (Fig. 12.6) [8].

**Radiopharmaceutical characteristics** Ammonia is a relatively small molecule with a molecular weight of 17.04. It exists in the blood predominantly in the form of the ammonium ion,  $\text{NH}_4^+$ .

**Extraction mechanism** Ammonia passes readily into the myocardial cells, mostly by passive diffusion of lipid-soluble ammonia across the cell membrane [8]. Inside the cell, ammonia converts to the ammonium ion, and then glutamine synthetase catalyzes the incorporation of ammonia into glutamic acid to form glutamine (Fig. 12.7). Because there is a large intracellular pool of glutamine and its turnover is slow, washout of N-13-labeled glutamine is slow [8].

**Extraction efficiency** The exact extraction efficiency is unknown but empirically appears to be high. The extraction efficiency of all myocardial perfusion radiopharmaceuticals falls off at higher coronary flow rates, i.e., the degree of localization of tracer in the myocardium is not a linear function of the blood flow. This phenomenon supports the fact that the images reflect clearance (Fig. 12.6) [8]. In addition, this means that the decreased blood flow to ischemic areas will be underestimated.

**Extraction mechanism, saturable or non-saturable** Non-saturable.

**Interventions** Image acquisition is done twice, once at rest and once following pharmacologic stress that significantly dilates normal coronary arteries. This maneuver reveals areas of coronary ischemia at stress that are not apparent at rest.

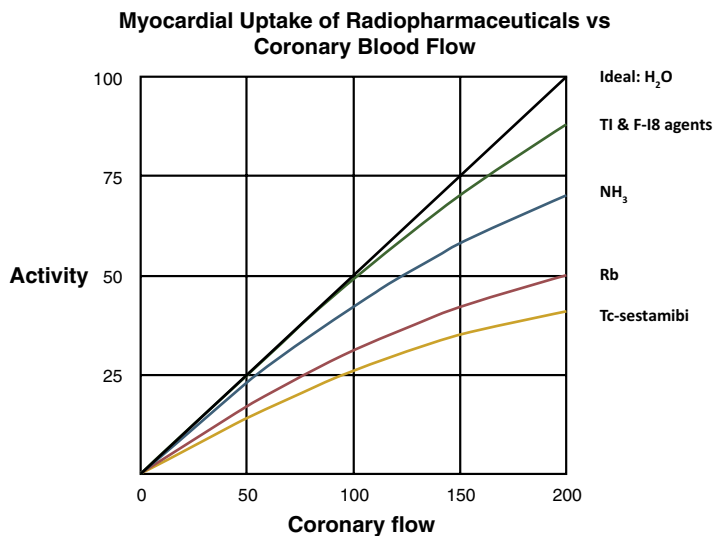


**Fig. 12.6** Myocardial uptake (clearance) of radiopharmaceuticals vs coronary blood flow. None of the radiopharmaceuticals that are used for measuring myocardial blood flow or perfusion are entirely accurate because they actually measure clearance and the extraction efficiency decreases as blood flow increases (From Schelbert [8], p. 403)

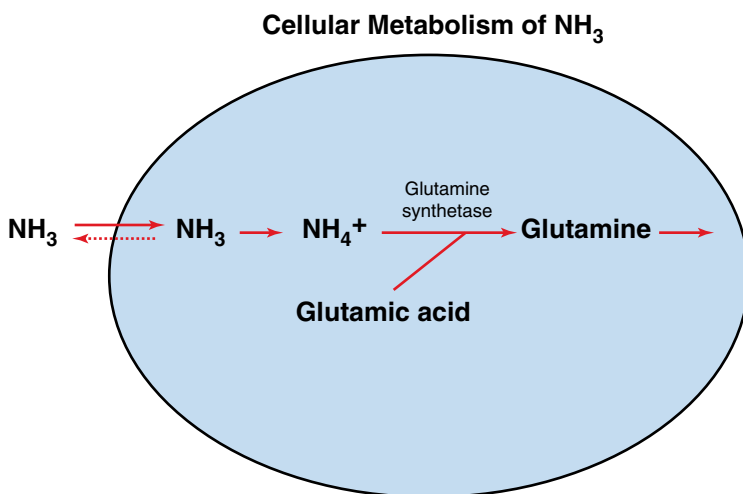


**Fig. 12.7** Cellular metabolism of NH<sub>3</sub>. N-13-ammonia diffuses freely through the capillary and cellular walls and then combines with glutamic acid to form glutamine, which traps the N-13 within the cell



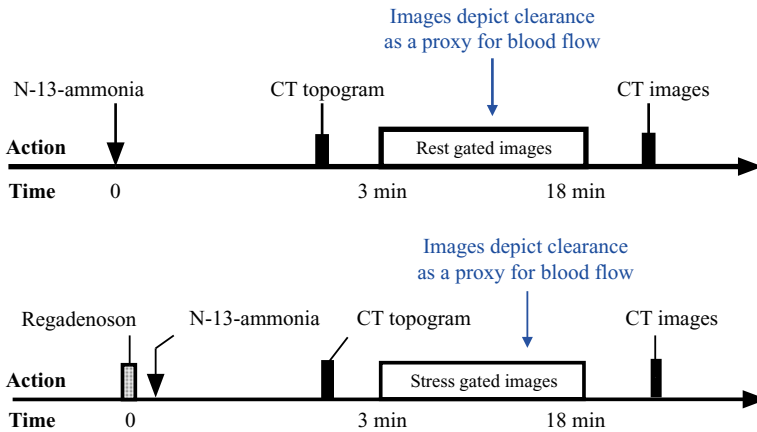


**Fig. 12.8** Protocol summary diagram

**Imaging** N-13 is a positron emitter so imaging is done with a PET-CT scanner. Because PET-CT images are tomographic, there is no need for background correction, and, since the CT images provide density maps for attenuation correction, no additional attenuation correction is required.

**Protocol design** Because of the short 10 min half-life of N-13, the stress acquisition can be begun as soon as 30 min after the rest acquisition with very little residual activity from the rest injection present in the stress images. The image acquisition process is gated for subsequent evaluation of left ventricular wall motion and ejection fraction (Fig. 12.8).

**Quantitative measurement: myocardial perfusion (clearance)** The myocardial activity is measured throughout the left ventricle based on the transaxial tomograms. The three-dimensional results are then displayed on a relative basis in a two-dimensional “bull’s-eye”. In the case of PET-CT, there is no need to secondarily correct for background activity or attenuation. The activity distribution in the left ventricle of an individual patient is compared to normal ranges on a gender-specific basis (Fig. 12.9) [9]. This is an example of quantitation of function on a relative basis (see Chap. 8, Quantitation of Function: Relative Measurement).

**Left ventricular ejection fraction: normal values** No separate normal ranges for males and females were identified in the literature. The listed reference consisted of six males and six females (Table 12.1) [10]. Females, in general, have a smaller left ventricle than males and a slightly higher ejection fraction.

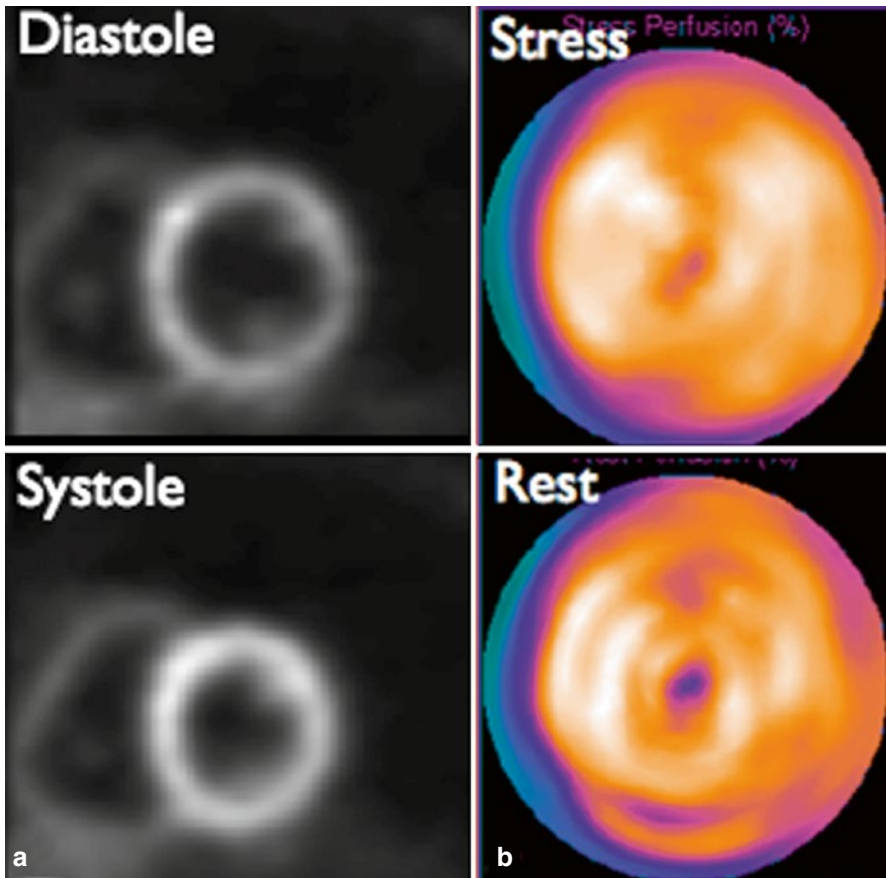


**Fig. 12.9** Normal transaxial tomograms and bull's-eye displays from a gated N-13-ammonia myocardial perfusion study. **(a)** Transaxial myocardial perfusion images from the mid-left ventricle at systole and diastole. Note that two left and one right papillary muscles are visible and that when the ventricles contract with systole, the walls thicken. **(b)** The counts in the left ventricle are displayed in “bull's-eye” mode on a pseudo-color scale with the apical counts at the center and the basilar counts at the periphery of the disk

### Myocardial Perfusion Study (Rb-82-Rubidium Chloride)

**Overview** The Myocardial Perfusion Study with Rb-82-rubidium is used to evaluate the distribution of blood flow and perfusion to the myocardium at rest and stress [11, 12]. In addition, the images are routinely gated to show regional wall motion and to allow calculation of the left ventricular ejection fraction [13].

However, despite the fact that the title of the study says “myocardial perfusion,” the images actually reflect myocardial clearance. This is true of all of the nuclear medicine studies that have the word “perfusion” in the title. Relative clearance will reflect relative perfusion or blood flow as long as the extraction efficiency is

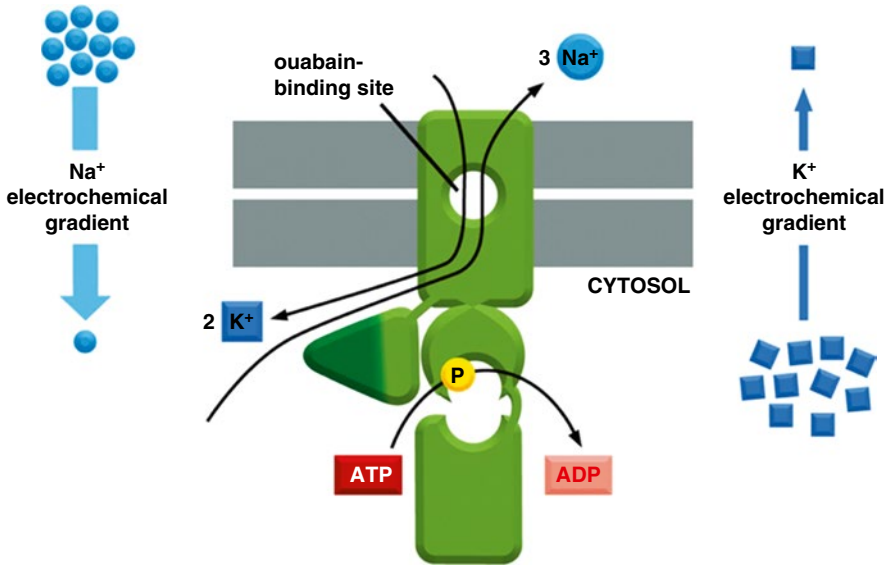


**Fig. 12.10** The Na<sup>+</sup>-K<sup>+</sup> pump. This transporter actively pumps Na<sup>+</sup> out and K<sup>+</sup> into the cell against their electrochemical gradients. For every molecule of ATP hydrolyzed inside the cell, three Na<sup>+</sup> are pumped out and two K<sup>+</sup> are pumped in (©Garland Science 2008)

uniform throughout the volume that is being imaged, but often it is not. For example, the extraction efficiency is higher in myocardium at low flow rates than at high flow rates (Fig. 12.6) [8].

**Radiopharmaceutical characteristics** Rubidium is a simple ion with a molecular weight of 85.47. It exists in the blood predominantly in the form of Rb<sup>+</sup>.

**Extraction mechanism** Rubidium-82 is a physiologic analog of potassium and is actively transported into cells via the sodium-potassium pump. The concentration of potassium in the cell is 10–30 times higher than outside the cell. Small amounts of rubidium-82 constantly leak out of the cell and then are pumped back in until an equilibrium is reached (Fig. 12.10).

**Extraction efficiency** The exact extraction efficiency is unknown but empirically appears to be high. The extraction efficiency of all myocardial perfusion radiopharmaceuticals falls off at higher coronary flow rates, i.e., the degree of localization of tracer in myocardium is not a linear function of blood flow [8]. This phenomenon supports the fact that the images reflect clearance (Fig. 12.6). In addition, this means that the decreased blood flow to ischemic areas will be underestimated.

**Extraction mechanism, saturable or non-saturable** Non-saturable.

**Interventions** Image acquisition is done twice, once at rest and once following pharmacologic stress that significantly dilates normal coronary arteries. This maneuver reveals areas of coronary ischemia at stress that are not apparent at rest.

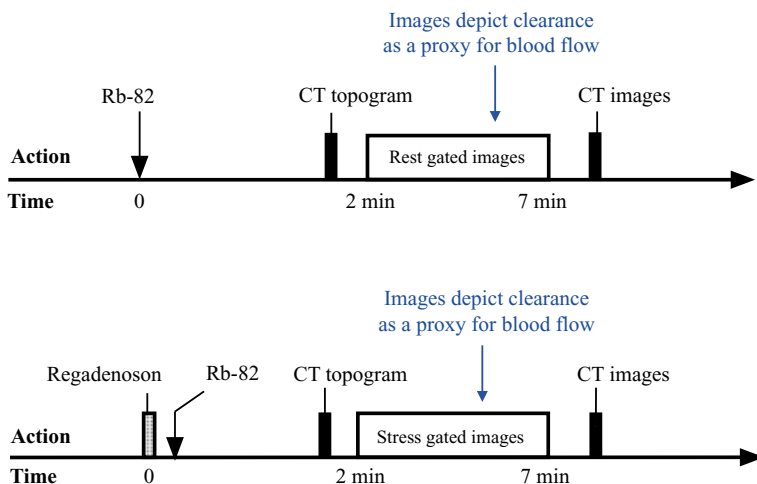


**Fig. 12.11** Protocol summary diagram

**Imaging** Rb-82 is a positron emitter so imaging is done with a PET-CT scanner. Because PET-CT images are tomographic, there is no need for background correction, and, since the CT images provide density maps for attenuation correction, no additional attenuation correction is required.

**Protocol design** Because of the short 75 s half-life of Rb-82, the stress acquisition can be started just 30 min after the rest acquisition with very little residual activity from the rest injection present in the stress images. The image acquisition process is gated for subsequent evaluation of left ventricular wall motion and ejection fraction (Fig. 12.11).

**Quantitative measurement: myocardial perfusion (clearance)** The myocardial activity is measured throughout the left ventricle based on the transaxial tomograms. The three-dimensional results are then displayed on a relative basis in a two-dimensional “bull’s-eye”. In the case of PET-CT, there is no need to secondarily correct for background activity or attenuation. The activity distribution in the left ventricle of an individual patient is compared to gender-specific normal range (Fig. 12.9b).

**Left ventricular ejection fraction: normal values** No normal ranges for males were identified. Females have a smaller left ventricle than males and a slightly higher ejection fraction (Table 12.1) [14].

## Myocardial Perfusion Study (Tc-99m-Sestamibi)

**Overview** The Myocardial Perfusion Study with Tc-99m-sestamibi is used to evaluate the distribution of blood flow and perfusion to the myocardium at rest and stress [15]. In addition, the images are routinely gated to show regional wall motion and to allow calculation of the left ventricular ejection fraction.

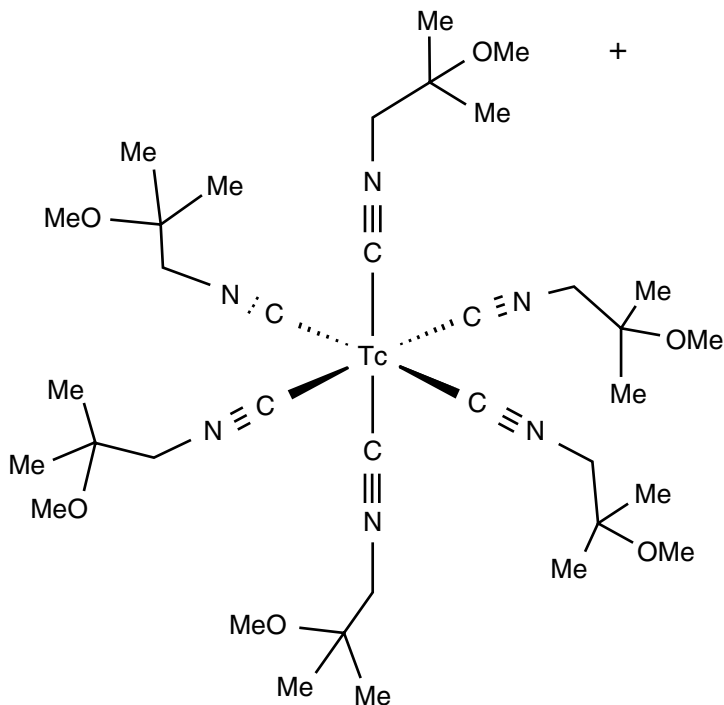


**Fig. 12.12** Chemical structure of Tc-99m-sestamibi. “Me” stands for methyl group, CH<sub>3</sub>. The radioisotope label, Tc-99m, is at the center

However, despite the fact that the title of the study says “myocardial perfusion,” the images actually reflect myocardial clearance. This is true of all of the nuclear medicine studies that have the word “perfusion” in the title. Relative clearance will reflect relative perfusion or blood flow as long as the extraction efficiency is uniform throughout the volume that is being imaged, but often it is not. For example, the extraction efficiency is higher in myocardium at low flow rates than at high flow rates (Fig. 12.4).

**Radiopharmaceutical characteristics** Tc-99m-sestamibi has a molecular weight of 777.69. Its molecular structure is shown in Fig. 12.12.

**Extraction mechanism** Tc-99m-sestamibi (methoxyisobutylisonitrile) is a lipophilic cationic complex that passively diffuses across the myocardial membrane and binds to proteins within the mitochondria [16]. The myocardial washout is slow with a half-time of 7 h.

**Extraction efficiency** The exact extraction efficiency is moderate at 38 % [16]. The extraction efficiency of all myocardial perfusion radiopharmaceuticals falls off at higher coronary flow rates, i.e., the degree of localization of tracer in myocardium is not a linear function of blood flow [8]. This phenomenon supports the fact that the myocardial images of the biodistribution of Tc-99m-sestamibi reflect clearance rather than blood flow or perfusion (Fig. 12.6). In addition, this means that the decreased blood flow to ischemic areas will be underestimated.

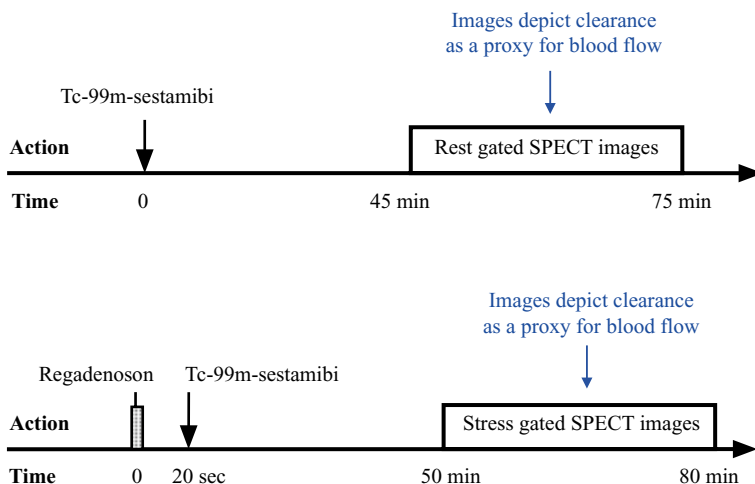


**Fig. 12.13** Protocol summary diagram

**Extraction mechanism: saturable or non-saturable** Non-saturable.

**Interventions** Image acquisition is done twice, once at rest and once following pharmacologic stress that significantly dilates normal coronary arterioles and causes up to a 500% increase in coronary blood flow [17]. This maneuver reveals areas of coronary ischemia at stress that are not apparent at rest.

**Imaging** Tc-99m-sestamibi is a single-photon emitter so imaging is done with a SPECT gamma camera. Because SPECT images are tomographic, there is no need for background correction. If imaging is done with SPECT-CT, the CT density maps allow a moderate degree of attenuation correction.

**Protocol design** Because of the relatively long half-life of Tc-99m-sestamibi, a 1-day rest and stress study requires that the second study is done with an administration of twice as much radiopharmaceutical as the first study so that the activity remaining from the first injection will be overwhelmed by the activity injected for the second acquisition. Usually, the rest study is done first and the stress study is done second. The image acquisition process is gated for subsequent evaluation of left ventricular wall motion and ejection fraction (Fig. 12.13).

**Quantitative measurement: myocardial perfusion (clearance)** The myocardial activity is measured throughout the left ventricle based on the transaxial tomograms. The three-dimensional results are then displayed on a relative basis in a two-dimensional “bull’s-eye”. In the case of SPECT-CT, there is no need to secondarily correct for background activity or attenuation. The activity distribution in the left ventricle of an individual patient is compared to normal ranges on a gender-specific basis (Fig. 12.9).

**Left ventricular ejection fraction: normal values** Females have a smaller left ventricle than males and a slightly higher ejection fraction (Table 12.1) [18–20]. In addition, the left ventricular ejection fraction increases with age for both males and females.

## Myocardial Perfusion and Viability Study (Tl-201-Thallos Chloride)

**Overview** The Myocardial Perfusion and Viability Study with Tl-201-thallos chloride is used to evaluate the distribution of perfusion in the myocardium at stress and viability at rest [21]. In addition, the images are gated to show regional wall motion and to allow calculation of the left ventricular ejection fraction.

However, despite the fact that the title of the study includes “myocardial perfusion,” the initial images actually reflect myocardial clearance. This is true of all of the nuclear medicine studies that have the word “perfusion” in the title. Relative clearance will reflect relative perfusion or blood flow as long as the extraction efficiency is uniform throughout the volume that is being imaged, but often it is not. For example, the extraction efficiency is higher in myocardium at low flow rates than at high flow rates, and the difference varies from one myocardial radiopharmaceutical to another (Fig. 12.6) [8].

**Radiopharmaceutical characteristics** Tl-201-thallos has a molecular weight of 204.37. It exists in the blood predominantly in the form of  $Tl^+$ .

**Extraction mechanism** The thallos ion behaves like  $K^+$  because they both have a single positive charge and similar ionic radii [9]. Thus,  $Tl^+$  is actively transported across the cell membrane by the Na-K pump (Fig. 12.10).

**Extraction efficiency** The exact extraction efficiency is moderate. The extraction efficiency of all myocardial perfusion radiopharmaceuticals falls off at higher coronary flow rates, i.e., the degree of localization of tracer in myocardium is not a linear function of blood flow. This phenomenon supports the fact that the myocardial images of the biodistribution of Tl-201-thallium reflect clearance rather than blood flow or perfusion (Fig. 12.6). This phenomenon supports the fact that the images reflect clearance (Fig. 12.6). In addition, this means that the decreased blood flow to ischemic areas will be underestimated.

**Extraction mechanism, saturable or non-saturable** Non-saturable.

**Interventions** Image acquisition is done twice, once at stress, either exercise or pharmacologic, and once approximately 3 h later at rest, so-called delayed images, for myocardial viability.

**Imaging** Tl-201 is a single-photon emitter so imaging is performed with a SPECT gamma camera. Because SPECT images are tomographic, there is no need for background correction. If imaging is done with SPECT-CT, the CT density maps allow a moderate degree of attenuation correction.

**Protocol design** The initial stress images demonstrate areas of ischemia at stress as well as areas that would also be ischemic at rest. However, the delayed images depict the distribution of viable myocardium even though it may be ischemic at rest. All viable myocardial cells have intact cell membranes and intact Na-K pumps so they will have normal potassium intracellular spaces. Thus, even cells that are ischemic at rest, but viable, will show thallium in the delayed images. This is the definition of hibernating myocardium. Without images of perfusion of myocardium at rest, it is not possible to differentiate hibernating myocardium (ischemic at rest, but viable) from stress ischemia (ischemic at stress, but normal perfusion at rest).

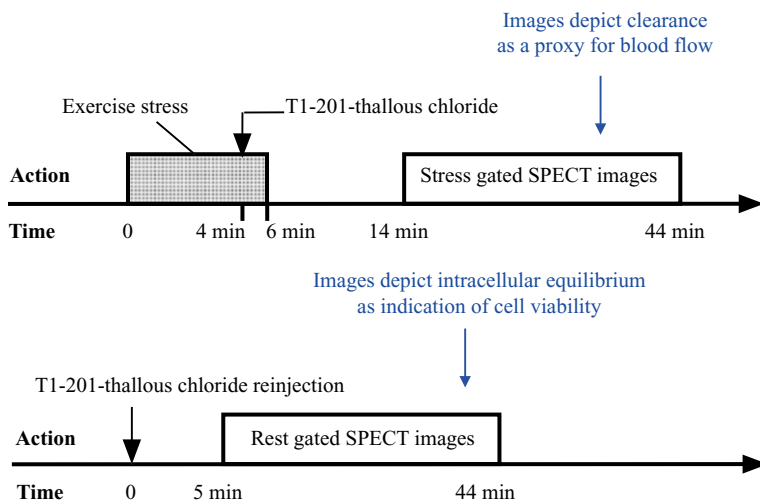


**Fig. 12.14** Protocol summary diagram

The image acquisition process is gated for subsequent evaluation of left ventricular wall motion and ejection fraction (Fig. 12.14).

**Quantitative measurement: myocardial perfusion (clearance)** The myocardial activity is measured throughout the left ventricle based on the transaxial tomograms. The three-dimensional results are then displayed on a relative basis in a two-dimensional “bull’s-eye” (Fig. 12.5b). In the case of SPECT-CT, there is no need to secondarily correct for background activity or attenuation. The activity distribution in the left ventricle of an individual patient is compared to normal ranges on a gender-specific basis [21–24].

**Left ventricular ejection fraction: normal values** Females have a smaller left ventricle than males and a slightly higher ejection fraction (Table 12.1) [3, 18].

## Myocardial Viability Study (F-18-Fluorodeoxyglucose)

**Overview** Normal myocardium generates energy by metabolizing either free fatty acids or glucose. The myocardium utilizes free fatty acids unless there is circulating insulin present, as in the case of a recent meal containing significant carbohydrates. In addition, ischemic, but viable, myocardium uses mainly glucose because it switches from aerobic to anaerobic metabolism. Infarcted myocardium takes up neither glucose nor free fatty acids. Thus, the F-18-Fluorodeoxyglucose (FDG) Myocardial Viability Study, performed in the fed state, will detect myocardium that is ischemic at rest, but still viable (hibernating myocardium), and differentiates hibernating myocardium from infarct [25, 26].



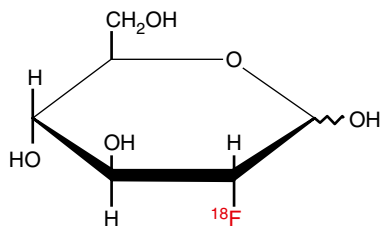


**Fig. 12.15** F-18-fluorodeoxyglucose (FDG). The hydroxyl group on the second carbon of glucose has been replaced by a positron-emitting fluorine-18 atom to form the radiopharmaceutical FDG

**Radiopharmaceutical characteristics** FDG has a molecular weight of 193.17, and the chemical structure is shown in Fig. 12.15. It exists in the blood predominantly in the form of soluble FDG.

**Extraction mechanism** FDG is transported across cell membranes by transmembrane glucose transporters (Fig. 12.16). There are two main classes: glucose transporters (GLUTs) and sodium-dependent glucose transporters (SGLTs). FDG binds mostly to GLUTs, which are not found in the renal tubular cells. This difference explains the lack of reabsorption of FDG from the tubular lumen. There are 11 subtypes of GLUT transporters. The primary one in cardiac muscle is the GLUT4 transporter, whose expression is regulated by the level of insulin in the blood (Fig. 12.17) [26, 27].

Once inside the cell, FDG is phosphorylated by the hexokinase enzyme (Fig. 12.18). The addition of a phosphate group to FDG prevents the radiopharmaceutical from diffusing out of the cell. At the same time, the absence of a hydroxyl group at the second-carbon position prevents phosphorylated FDG from binding to the next enzyme in the glycolytic pathway. This fact prevents FDG from being metabolized and, in turn, prevents the radiolabel, F-18, from diffusing back out of the cell into the blood.

While differences in the metabolic behavior of FDG compared to native glucose make it an imperfect tracer of glucose, the differences actually improve FDG from an imaging point of view. If F-18 diffused back out of the cells, the contrast between cells that clear FDG and background including blood would be decreased. In addition, if FDG were reabsorbed by the kidneys, there would be a greater amount of FDG in the blood and again the contrast between cells that clear FDG and background would be decreased.

**Extraction efficiency** The exact extraction efficiency varies from organ to organ, and in some organs, i.e., heart, it depends greatly on whether there is insulin in the blood or not. In addition, as stated above, hypoxia, usually due to ischemia, increases the uptake of glucose and FDG in the myocardium.

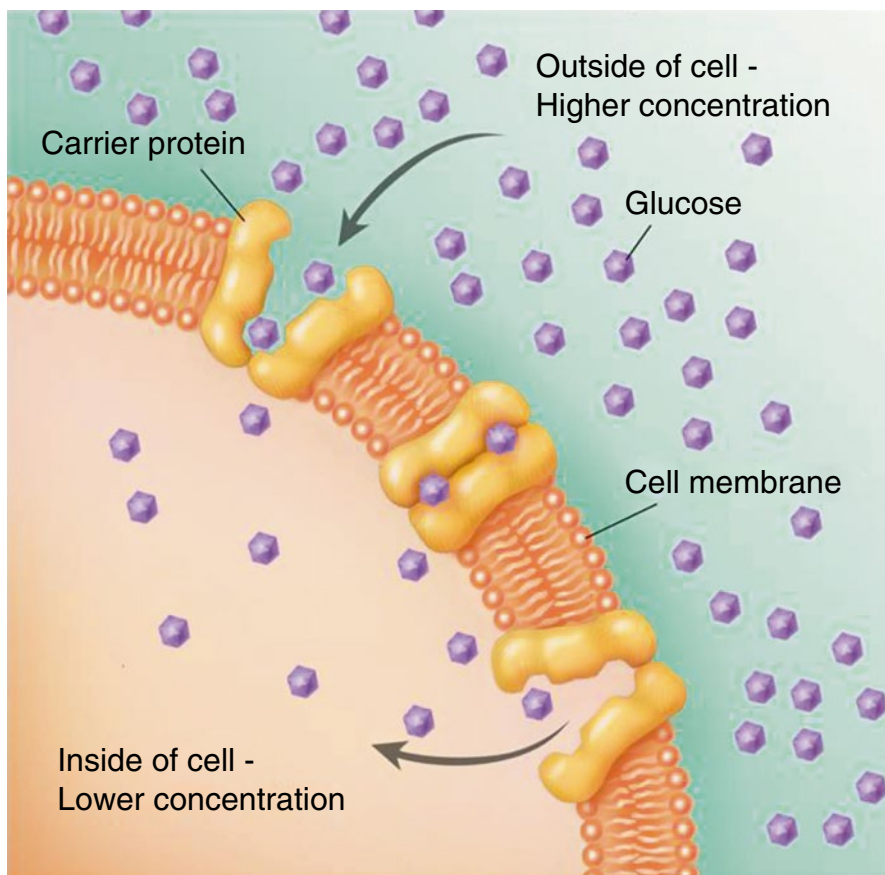


**Fig. 12.16** Transport of glucose across the cell membrane by GLUT. GLUT transporters are an example of passive facilitative transport which is driven by the concentration gradient of glucose. The gradient is maintained by the intracellular phosphorylation of glucose. When glucose binds to the GLUT transporter, it induces a change in configuration of the transporter which transports the glucose across the cell membrane and causes the release of the glucose molecule in the intracellular space

**Extraction mechanism saturable or non-saturable** Saturable. Hyperglycemia increases competition for glucose receptors and decreases clearance of FDG. In addition, hyperglycemia can cause a downregulation of the GLUT receptors, e.g., GLUT4, so that not only is there an increase in nonradioactive glucose molecules for binding to the GLUT receptors, but there are fewer receptors (Fig. 12.17).

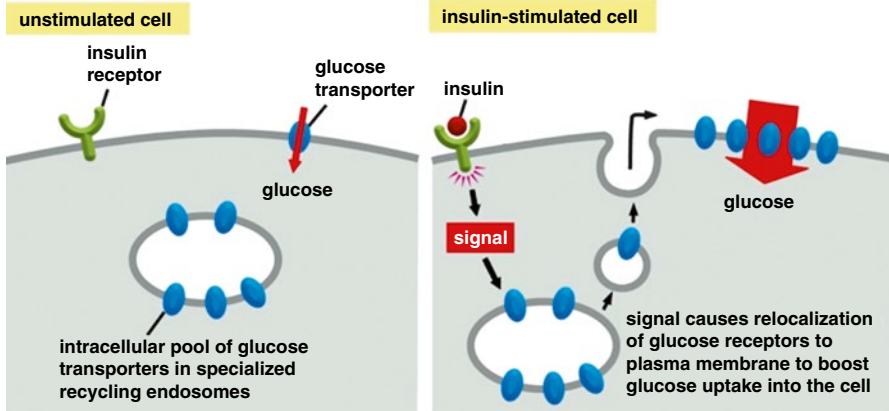


**Fig. 12.17** Insulin regulation of cell membrane expression of GLUT4. GLUT4 is one of a family of passive facilitative glucose transporters. It is expressed in the cell membrane in response to the blood level of insulin. For the Myocardial Viability Study with FDG, the patient must be prepared with a high-carbohydrate meal to ensure that there will be circulating insulin at the time of FDG injection (©Garland Science 2008)

### Cellular Metabolism of FDG

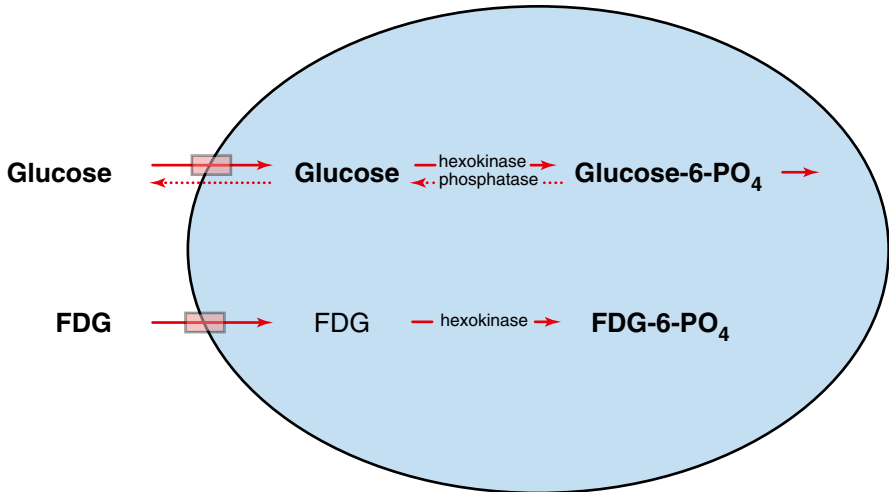


**Fig. 12.18** Cellular uptake of glucose vs FDG. Most transmembrane glucose transport proteins bind to glucose and FDG equally. In addition, the hexokinase enzyme binds to and phosphorylates glucose and FDG equally well. However, the next enzyme in the glycolytic pathway binds phosphorylated glucose, but not phosphorylated FDG

**Interventions** The patient is instructed to eat a high-carbohydrate meal 2 h before injection of the radiopharmaceutical to ensure that there is some insulin in the blood. The postprandial carbohydrate meal increases the blood glucose level, which, in

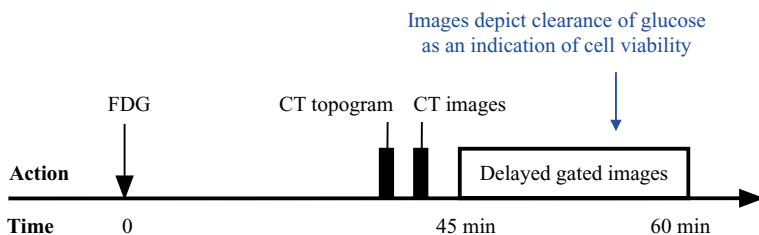


**Fig. 12.19** Protocol summary diagram

turn, increases the blood insulin level. Increased blood insulin increases the GLUT4 expression and clearance rate in myocardial cells significantly.

**Imaging** F-18 is a positron emitter so imaging is done with a PET-CT scanner. Because the PET images are tomographic, there is no need for background correction. And because the CT images provide high-resolution density maps, the images are corrected for attenuation.

**Protocol design** The high-carbohydrate meal 2 h prior to injection of the FDG is critical. Without insulin in the blood, there may be no uptake or clearance of FDG by the myocardium or even patchy uptake which can be confusing.

The image acquisition process is gated for subsequent evaluation of the left ventricular wall motion and ejection fraction (Fig. 12.19).

**Quantitative measurement: myocardial viability** The myocardial activity is measured throughout the left ventricle based on the transaxial tomograms. The three-dimensional results are then displayed on a relative basis in a two-dimensional “bull’s-eye”. In the case of PET-CT, there is no need to secondarily correct for background activity or attenuation. The activity distribution in the left ventricle of an individual patient is compared to normal ranges on a gender-specific basis.

**Left ventricular ejection fraction: normal values** Normal values for the left ventricular ejection fraction could not be identified, but are probably similar to those listed for Tc-99m-sestamibi at rest. Females have a smaller left ventricle than males and a slightly higher ejection fraction (Table 12.1).

## References

### Cardiac Gated Blood Pool Study (Tc-99m-Red Blood Cells)

1. Freedman JC. Cell membranes. In: Sperelakis N, editor. Cell physiology sourcebook: essentials of membrane biophysics. 4th ed. London: Academic Press; 2012. p. 49.
2. Massardo T, Jaimovich R, Lavados H, et al. Comparison of radionuclide ventriculography using SPECT and planar techniques in different cardiac conditions. *Eur J Nucl Med Mol Imaging*. 2007;34:1735–46.
3. Berman DS, Maddahi J, Garcia EV, et al. Assessment of left and right ventricular function with multiple gated equilibrium cardiac blood pool scintigraphy. In: Berman DS, Mason DT, editors. *Clinical nuclear cardiology*. New York: Grune & Stratton; 1981. p. 247.
4. Jackson SA, Nickerson R, Martin RH, et al. Factors of variability in the radionuclide evaluation of global and regional left ventricular ejection fraction. *J Nucl Med Technol*. 1991;19:77–80.
5. Corbett JR, Akinboboye OO, Bacharach SL, et al. ASNC imaging guidelines for nuclear cardiology procedures. *J Nucl Cardiol*. 2008.

### **Lymphoscintigraphy (Filtered Tc-99m-Sulfur Colloid)**

6. Goldfarb LR, Alazraki NP, Eshima D, et al. Lymphoscintigraphic identification of sentinel lymph nodes: clinical evaluation of 0.22  $\mu\text{m}$  filtration of Tc-99m sulfur colloid. *Radiology*. 1998;208:505–9.
7. Nopajaroonsri C, Simon GT. Phagocytosis of colloidal carbon in a lymph node. *Am J Pathol*. 1971;65:25–42.

### **Myocardial Perfusion Study (N-13-Ammonia)**

8. Schelbert HR. Positron emission tomography of the heart: methodology, findings in the normal and disease heart, and clinical applications. In: Phelps ME, editor. *PET: molecular imaging and its clinical applications*. New York: Springer; 2004. p. 402–3.
9. Eisner RL, Tamas MJ, Coninger K, et al. Normal SPECT thallium-201 bull's-eye display: gender differences. *J Nucl Med*. 1988;29:1901–9.
10. Hickey KT, Sciacca R, Sabahat B, et al. Assessment of cardiac wall motion and ejection fraction with gated PET using N-13 ammonia. *Clin Nucl Med*. 2004;29:243–8.

### **Myocardial Perfusion Study (Rb-82-Rubidium Chloride)**

11. Santana CA, Folk RD, Garcia EV, et al. Quantitative Rb-82 PET-CT: development and validation of myocardial perfusion database. *J Nucl Med*. 2007;48:1122–8.
12. Fakhri GE, Kardan A, Sitek A, et al. Reproducibility and accuracy of quantitative myocardial blood flow assessment with Rb-82 PET: comparison with N-13-ammonia PET. *J Nucl Med*. 2009;50:1062–71.
13. Chander A, Brenner M, Lautamaki R, et al. Comparison of measures of left ventricular function from electrocardiographically gated Rb-82 PET with contrast-enhanced CT ventriculography: a hybrid PET-CT analysis. *J Nucl Med*. 2008;49:1643–50.
14. Bravo PE, Chien D, Javadi M, et al. Reference ranges for LVEF and LV volumes from electrocardiographically gated Rb-82 cardiac PET-CT using commercially available software. *J Nucl Med*. 2010;51:898–905.

### **Myocardial Perfusion Study (Tc-99m-Sestamibi)**

15. Zanco P, Zampiero A, Favero A, et al. Myocardial technetium-99m sestamibi single-photon emission tomography as a prognostic tool in coronary artery disease: multivariate analysis in a long-term prospective study. *Eur J Nucl Med*. 1995;22:1023–8.
16. Gopal BS. Tc-99m-labeled radiopharmaceuticals. In: Gopal BS, editor. *Fundamentals of nuclear pharmacy*. New York: Springer; 2010. p. 124.
17. Duncker DJ, Bache RJ. Regulation of coronary blood flow during exercise. *Physiol Rev*. 2008;88:1009–86.
18. Ababneh AA, Sciacca RR, Kim B, et al. Normal limits for left ventricular ejection fraction and volumes estimated with gated myocardial perfusion imaging in patients with normal exercise test results: influence of tracer, gender, and acquisition camera. *J Nucl Cardiol*. 2000;7:661–8.
19. Rozanski A, Nicholes K, Yao SS, et al. Development and application of normal limits for left ventricular ejection fraction and volume measurements from Tc-99m-sestamibi myocardial perfusion gated SPECT. *J Nucl Med*. 2000;41:1445–50.
20. De Bondt P, Van de Wiele C, De Sutter J, et al. Age- and gender-specific differences in left ventricular cardiac function and volumes determined by gated SPET. *Eur J Nucl Med*. 2001;28:620–4.

### **Myocardial Viability Study (TI-201-Thallos Chloride)**

21. Schafers M, Matheja P, Hasfeld M, et al. The clinical impact of thallium-201 reinjection for the detection of myocardial hibernation. *Eur J Nucl Med.* 1996;23:407–13.
22. Eisner RL, Tamas MJ, Coninger K, et al. Normal SPECT thallium-201 bull's-eye display: gender differences. *J Nucl Med.* 1988;29:1901–9.
23. Garcia EV, DePuey G, Sonnemaker RE, et al. Quantification of the reversibility of stress-induced thallium-201 myocardial perfusion defects: a multicenter trial using bull's-eye polar maps and standard normal limits. *J Nucl Med.* 1990;31:1761–5.
24. Yamagishi H, Shirai N, Yoshiyama M, Teragaki M, et al. Incremental value of left ventricular ejection fraction for detection of multivessel coronary artery disease in exercise TI-201 gated myocardial perfusion imaging. *J Nucl Med.* 2002;43:131–9.

### **Myocardial Viability Study (F-18-Fluorodeoxyglucose)**

25. Schelbert HR. F-18-deoxyglucose and the assessment of myocardial viability. *Semin Nucl Med.* 2002;32:60–9.
26. Abraham A, Nichol G, Williams KA, et al. F-18-FDG PET imaging of myocardial viability in an experienced center with access to F-18-FDG and integration with clinical management teams: the Ottawa-FIVE substudy of the PARR 2 trial. *J Nucl Med.* 2010;51:567–74.
27. Wood IS, Trayhurn P. Glucose transporters (GLUT and SGLT): expanded families of sugar transport proteins. *Br J Nutr.* 2003;89:3–9.